Received: 24 July 2019 | Revised: 12 February 2020 | Accepted: 18 February 2020

DOI: 10.1096/fj.201901852RR

RESEARCH ARTICLE

THE FASEB JOURNAL

Discoidin domain receptor 1 regulates endochondral ossification through terminal differentiation of chondrocytes

Liang-Yin Chou[1,2,3] | Chung-Hwan Chen[2,3,4,5,6,7] | Yi-Hsiung Lin[8,9,10] | Shu-Chun Chuang[2,3] | Hsin-Chiao Chou[1,2,3] | Sung-Yen Lin[1,2,3,4,5] | Yin-Chi Fu[1,2,3,4] | Je-Ken Chang[2,3,5,7] | Mei-Ling Ho[1,2,3,4,11,12] | Chau-Zen Wang[1,2,3,11,13]

[1]Graduate Institute of Medicine, College of Medicine, Kaohsiung Medical University, Kaohsiung, Taiwan

[2]Orthopaedic Research Centre, Kaohsiung Medical University, Kaohsiung, Taiwan

[3]Regeneration Medicine and Cell Therapy Research Center, Kaohsiung Medical University, Kaohsiung, Taiwan

[4]Department of Orthopedics, College of Medicine, Kaohsiung Medical University, Kaohsiung, Taiwan

[5]Department of Orthopedics, Kaohsiung Municipal Ta-Tung Hospital, Kaohsiung Medical University, Kaohsiung, Taiwan

[6]Institute of Medical Science and Technology, National Sun Yat-Sen University, Kaohsiung, Taiwan

[7]Division of Adult Reconstruction Surgery, Department of Orthopedics, Kaohsiung Medical University Hospital, Kaohsiung Medical University, Kaohsiung, Taiwan

[8]Department of Biotechnology, Kaohsiung Medical University, Kaohsiung, Taiwan

[9]Division of Cardiology, Department of Internal Medicine, Kaohsiung Medical University Hospital, Kaohsiung, Taiwan

[10]Lipid Science and Aging Research Center, Kaohsiung Medical University, Kaohsiung, Taiwan

[11]Department of Physiology, College of Medicine, Kaohsiung Medical University, Kaohsiung, Taiwan

[12]Department of Marine Biotechnology and Resources, National Sun Yat-sen University, Kaohsiung, Taiwan

[13]Department of Medical Research, Kaohsiung Medical University Hospital, Kaohsiung, Taiwan

Correspondence
Chau-Zen Wang and Mei-Ling Ho, Department of Physiology, College of Medicine, and Graduate Insititute of Medicine, College of Medicine, Kaohsiung Medical University, No. 100, Shih-Chuan 1st Road, Kaohsiung 807, Taiwan.
Email: czwang@kmu.edu.tw (C.-Z. W) and homelin@kmu.edu.tw (M.-L. H)

Funding information
Ministry of Science and Technology (MOST), Grant/Award Number: MOST108-2320-B-037-008 and MOST108-2314-B-037-059-MY3; Kaohsiung Medical University, Grant/Award Number: KMU-TP-105B10, KMU-DK105009, KMU-TC108A02 and KMU-TC108A02-1

Abstract

Chondrocytes in growth plates are responsible for longitudinal growth in long bones during endochondral ossification. Discoidin domain receptor 1 (*Ddr1*) is expressed in chondrocytes, but the molecular mechanisms by which DDR1 regulates chondrocyte behaviors during the endochondral ossification process remain undefined. To elucidate *Ddr1*-mediate chondrocyte functions, we generated chondrocyte-specific *Ddr1* knockout (CKOΔ*Ddr1*) mice in this study. The CKOΔ*Ddr1* mice showed delayed development of the secondary ossification center and increased growth plate length in the hind limbs. In the tibial growth plate in CKOΔ*Ddr1* mice, chondrocyte proliferation was reduced in the proliferation zone, and remarkable downregulation of Ihh, MMP13, and Col-X expression in chondrocytes resulted in decreased terminal differentiation in the hypertrophic zone. Furthermore, apoptotic chondrocytes

Abbreviations: 4-OHT, 4-hydroxytamoxifen; ALP, alkaline phosphatase; BV/TV, bone volume to total volume; CKOΔ*Ddr1* mice, chondrocyte-specific *Ddr1* knockout mice; Col-X, type X collagen; DDR1, discoidin domain receptor 1; HZ, hypertrophic zone; Ihh, Indian hedgehog; micro-CT, microcomputed tomography; MMPs, matrix metalloproteinases; PZ, proliferation zone; Runx2, Runt-related transcription factor 2; SOCs, secondary ossification centers; Tb, N, trabecular number; Tb, Sp, trabecular separation; Tb, Th, trabecular thickness; VEGF, vascular endothelial growth factor.

Liang-Yin Chou and Chun-Hwan Chen are first authors to the study.

© 2020 Federation of American Societies for Experimental Biology

were reduced in the growth plates of CKOΔ*Ddr1* mice. We concluded that chondrocytes with *Ddr1* knockout exhibit decreased proliferation, terminal differentiation, and apoptosis in growth plates, which delays endochondral ossification and results in short stature. We also demonstrated that *Ddr1* regulates the Ihh/Gli1/Gli2/Col-X pathway to regulate chondrocyte terminal differentiation. These results indicate that *Ddr1* is required for chondrocytes to regulate endochondral ossification in skeletal development.

KEYWORDS

chondrocytes, DDR1, discoidin domain receptor 1, endochondral ossification, skeletal development

1 | INTRODUCTION

During embryonic and postnatal skeletogenesis, there are two skeletal ossification processes: endochondral ossification and intramembranous ossification. During endochondral ossification, chondrocytes are differentiated from mesenchymal stem cells, and then, undergo terminal differentiation and apoptosis. The cartilage is replaced with bone, which is then remodeled by osteoblasts and osteoclasts. During intramembranous ossification, mesenchymal stem cells directly differentiate into osteoblasts.[1] Multiple factors in chondrogenesis regulate endochondral ossification. Sox9 is an essential transcription factor to commit mesenchymal stem cells into chondroprogenitor cells and is also expressed at both the growth plate and articular cartilage.[2] Additionally, Sox9 also inhibits Runt-related transcription factor 2 (Runx2) expression to prevent osteogenesis.[3,4] The other factors expressed by chondrocytes during terminal differentiation include type X collagen (Col-X), matrix metalloproteinases (MMPs), Indian hedgehog (Ihh), and caspase 3.[5-9] However, if the endochondral ossification process is disturbed, chondrodysplasia caused short stature may occur.[10]

The collagen-binding transmembrane proteins discoidin domain receptors (DDRs) belong to a distinct class of receptor tyrosine kinases and have two subfamilies, DDR1 and DDR2.[1,11] DDRs regulate a wide range of cellular functions, such as proliferation, differentiation, apoptosis, and extracellular matrix homeostasis/remodeling.[12] Although DDR1 and DDR2 exhibit some amino acid sequence similarity,[12,13] their cellular functions are distinct, especially in bone and cartilage.[12-15] DDR1 is activated by collagen types I-V, VIII, and X, whereas DDR2 is activated mainly by fibrillary collagen types I–III, V, and X.[1,16,17] DDR1 is expressed in chondrocytes.[18] However, whether DDR1 mediates the signal from type II collagen and the molecular mechanisms by which DDR1 regulates chondrocyte behaviors during the endochondral ossification process remain unclear. This incomplete knowledge is partly due to the paucity of studies using tissue-specific knockouts of *Ddr1* expression.[15] A tissue-specific *Ddr1* knockout model using the Cre/loxP-mediated recombination system offers an alternative approach and a more reliable phenotype. In this study, we originally created chondrocyte-specific *Ddr1* knockout mice (CKOΔ*Ddr1* mice) to evaluate the roles of DDR1 in the molecular and cellular processes of chondrocytes during skeletal development. Our results showed that *Ddr1* is required for regulating the proliferation, terminal differentiation, and apoptosis of chondrocytes during endochondral ossification in skeletal development.

2 | MATERIALS AND METHODS

2.1 | Chondrocyte-specific (a1(II) collagen CreERT;*Ddr1*$^{f/f}$ mice; CKO mice) *Ddr1* knockout mice

All animal studies were approved by the Kaohsiung Medical University Animal Care and Use Committee (105127). To generate conditional *Ddr1* floxed mice (*Ddr1*$^{f/f}$) with a floxed exon 2 and exon 12 at the DDR1 locus (Figure 1A), targeting vectors (Pl253) harboring floxed *Ddr1* sites, and the neomycin resistance (NeoR) cassette were electroporated into embryonic stem (ES) cells derived from the 129P2 background. ES cells containing the floxed *Ddr1* allele were injected into blastocysts of the C57BL/6 embryos to generate chimeric mice, and the offspring were crossed with flippase transgenic mice to remove the NeoR cassette, which was flanked by flippase recombinase target (FRT) sequences. The hybrid mice were backcrossed to the C57BL/6 strain for 12 generations. The inducible a1(II)-collagen-CreERT cassette contains a 1-kb proximal fragment of the Col2a1 promoter, a β-globin intron (IVS), SV40 polyA, and the Col2a1enhancer (Figure S1A). To generate a1(II)CreERT;*Ddr1*$^{f/f}$ mice, *Ddr1*$^{f/f}$ mice were crossed with a1(II)collagenCreERT mice.[19] Genotyping was performed by polymerase chain reaction (PCR) using tail genomic DNA. The presence of the 3′ loxP site was verified by PCR using the primer pair 5′-ATAGCGGCCGCTGCTGGTCTTAGCTCTGT-3′ and

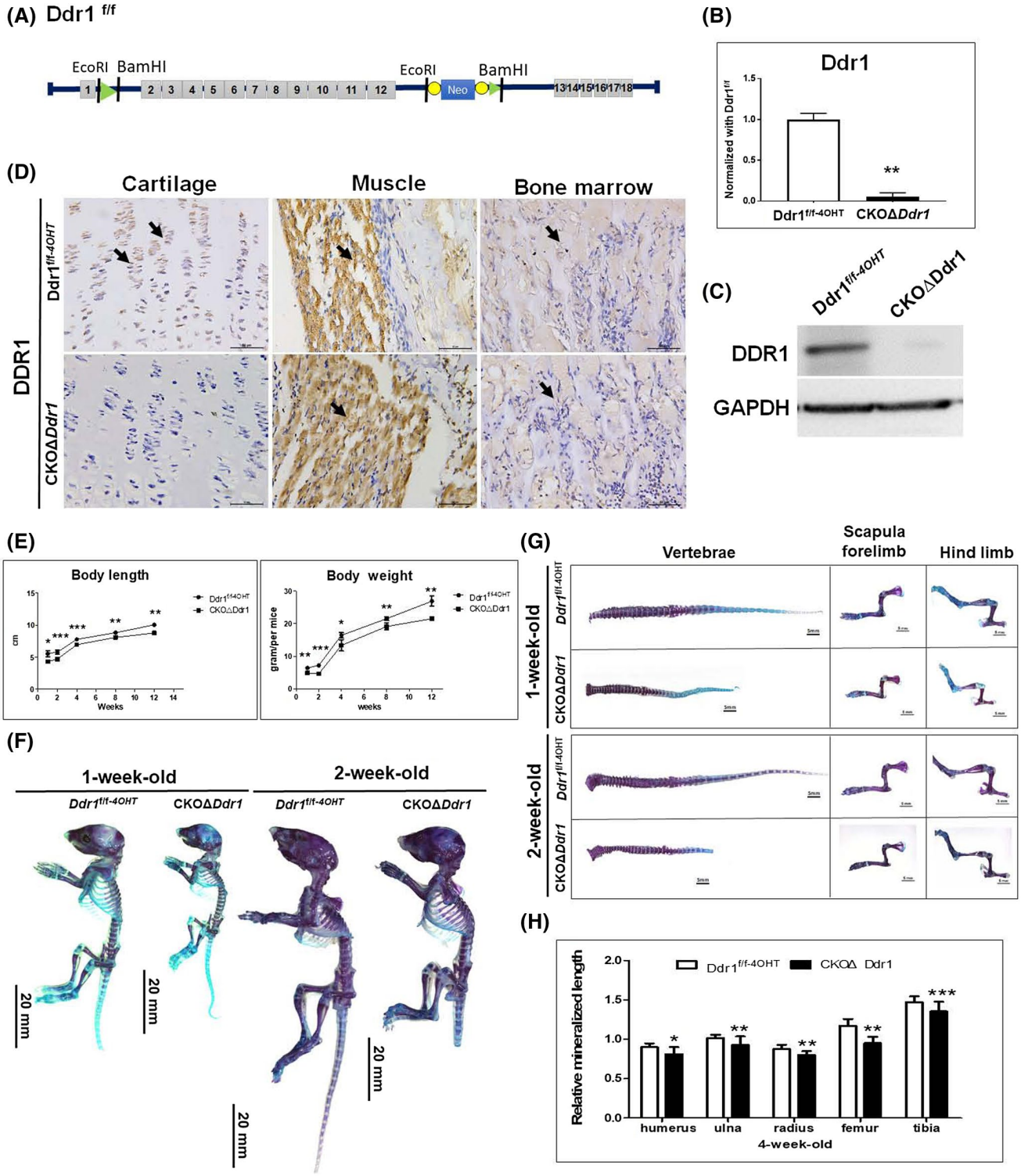

FIGURE 1 Skeletal dysplasia of chondrocyte-specific (a1(II) collagen CreERT;*Ddr1*$^{f/f}$ mice) CKOΔ*Ddr1* mice. A, Schematic of conditional *Ddr1* transgenic mice (*Ddr1*$^{f/f}$). The articular cartilage of long bones from P4-P5 was assessed for (B) *Ddr1* gene expression and (C) DDR1 protein level normalized to GAPDH. D, IHC staining of DDR1 in tibia; cartilage (arrow), muscle (arrow), and bone marrow (arrow) in 1-week-old *Ddr1*$^{f/f}$-4OHT and CKOΔ*Ddr1* mice. Each group, N ≥ 8. E, Quantitation of 1-, 2-, 4-, 8-, and 12-week-old body length and body weight. F, Double staining of the overall body of 1- and 2-week-old mice. G, Endochondral formation, including vertebrae, scapula/forelimb, and hind limb. H, Quantitation of long bone length. Each group, N ≥ 6; the data represent the mean ± SE by Student's *t* test; $^{**}P \leq .01$, $^{***}P \leq .001$

5′-ATAGTCGACACAGAGAGTTAAGCCAGA-3′); the Cre site was verified with the primer pair 5′-GCGGTCTGG CAGTAAAAACTATC-3′and5′-GTGAAACAGCATTGCT GTCACTT-3′. The wild-type (WT) and floxed alleles yielded 630 and 730 bp products, respectively. *Ddr1* protein expression in chondrocytes from a1(II)Cre; $Ddr1^{f/f}$ mice was detected.

2.2 | 4-Hydroxytamoxifen administration

The Cre-LoxP system requires the injection of 4-hydroxytamoxifen (4-OHT) to activate Cre recombinase. A stock of 4-OHT (T5648, Sigma-Aldrich, St. Louis, MO, USA) was prepared by dissolving 50 mg of powder in 50 μL of DMSO and shaking overnight. The working concentration was dissolved in corn oil (C8267, Sigma-Aldrich, St. Louis, MO) at a 9:1 ratio of oil:DMSO mixture to 4 mg/kg of mouse weight. 4-OHT was intraperitoneally injected 4 mg/kg/once on day 14.5 with progesterone 2 mg/kg (P0130, Sigma-Aldrich, St. Louis, MO) after birth collected 1-week-old perinatal mice. Collected postnatal 2 and 4-week-old mice were injected with 4 mg/kg/once a week. The experiment groups were treated as follows: $Ddr1^{f/f\text{-}4OHT}$ (as control) and CKOΔ*Ddr1 male mice both treated with 4-OHT*. Each group containing six animals.

2.3 | Cell culture and inhibitor treatment

The human articular chondrocyte (HAC) cell line was purchased from Lonza Walkersville Inc (CC-2550; Lonza Walkersville Inc), the cell culture at a density of 4×10^5 in 75 cm^2 flasks with the CBM Chondrocyte Growth Basal Medium (CC3217; Lonza Walkersville Inc) contained R3-IGF-1, bFGF, 1% of insulin-transferrin-selenium, insulin, 10% of fetal bovine serum (FBS), and gentamicin/amphotericin-B. The cell line was cultured at 37°C in a humidified 5% of CO_2 incubator. The human chondrosarcoma cell line SW1353 (HTB-94) (ATCC, Manassas, VA, USA) was grown in Leibovitz's L15 medium with 10% of FBS, 100 units/mL penicillin, and 100 μg/mL antimycoplasma. The SW1353 cells were maintained at 37°C without CO_2. The inhibitor HPI-4 (Ciliobrevin A, Selleckchem, Houston, USA) inhibits sonic hedgehog (Shh) and downstream Smo pathway activation. The stock of HPI-4 was prepared by dissolving in DMSO at a concentration of 10 mM and stored at −80°C. SW1353 cells were seeded at 2×10^5 cell/cm^2 in a 6-cm dish and treated with 10 μM of HPI-4 for 24 hours. Protein levels were then assessed by western blot.

2.4 | Lentivirus constructs and transfection

Transient *Ddr1* knockdown and overexpression were achieved with lentivirus in SW1353 cells. Lentivirus particles expressing shLacZ (knockdown *Ddr1* control), shDdr1 (knockdown *Ddr1*, TRCN0000010084), vehicle plasmid (overexpression control, TRC005), and ovDdr1 (overexpression *Ddr1*, TRCN0000288589) were purchased from the RNAi Core Facility of Taiwan. SW1353 cells and HAC cells were cultured in 6-well plates at a density of 2×10^5, infected with lentivirus particles (MOI of 1), and cultured for 16 hours. Stable cell lines were selected by puromycin (2 μg/mL) resistance and used in western blot analysis.

2.5 | Double staining analysis for skeleton

$Ddr1^{f/f\text{-}4OHT}$and CKOΔ*Ddr1* mice were euthanized by CO2. The skins were removed, and the mice were eviscerated and then fixed in 4% of paraformaldehyde for 24 hours. Next, the mice were soaked in 2% of Alcian Blue 8GX (A5268, Sigma-Aldrich) until the cartilaginous matrix of skeletons became blue. Then, the cells were washed with 0.5% of KOH (60377, Sigma-Aldrich, St. Louis, MO, USA) until the muscle became transparent. After the bones were washed in ddH_2O for 2 days and soaked in 1% of Alizarin red S (A5533, Sigma-Aldrich, St. Louis, MO, USA) for 15 minutes, they became purple. The specimens were washed in KOH until the muscle was transparent and were observed under a Leica-DSM1000 microscope (Leica Microsystems, Wetzlar, Germany).

2.6 | Microcomputed tomography

The 3-D reconstructions of the tibia were procured via high resolution microcomputed tomography (micro-CT) analysis (SkyScan 1076; SkyScan NV, Kontich, Belgium). Tibiae were scanned at an isotropic voxel resolution of 9 μm, without a filter, 44 kV X-ray tube voltage, 222 μA tube electric current, and 1150 ms scanning exposure time. The 3-D images were reconstructed for analysis using a scale of 0-0.09 (NRecon version 1.6.1.7; SkyScan NV, Kontich, Belgium), and the 3-D morphometric parameters of the tibia were computed using a direct 3D, total length was 5.0-mm for 3D structure and coronal section; beneath growth plate 5.0-mm to 7.0-mm as region for 3D cortical structure; beneath growth plate 0.5-mm to 2.5-mm as region for 3D trabecular structure and reign of interest (ROI; 4-mm circle; 100 cuts) analysis for the trabecular quantitation; these parameters included percent bone volume to total volume (BV/TV, %), trabecular thickness (Tb.Th, μm), trabecular number (Tb.N, mm-1), and trabecular separation (Tb.Sp, μm).

2.7 | Histomorphometric analysis

Harvested tibiae were fixed in 4% of paraformaldehyde solution, demineralized at 4°C using 0.5 M of

ethylenediaminetetraacetic acid, embedded in paraffin, and then sectioned at a thickness of 5 μm. The sections were histologically analyzed by staining with hematoxylin (H3136, Sigma-Aldrich, St. Louis, MO, USA) and eosin (318906, Sigma-Aldrich, St. Louis, MO, USA) or assessed for GAG content using 0.1% of Safranin O red (HT90432, Sigma-Aldrich, St. Louis, MO, USA) and 0.05% of Fast Green (2353-45-9, Sigma-Aldrich, St. Louis, MO, USA). Stained specimens were observed with a Leica-DM1000 microscope (Leica Microsystems, Wetzlar, Germany).

2.8 | Immunohistochemistry

Tibia sections were deparaffinized and rehydrated. Antigen retrieval was performed by incubating the sections in 100°C 0.1% EDTA in 1X PBS for 30 minutes. After three 5-minutes washes in 1X PBS, a mouse/rabbit probe HRP labeling kit (BIOTNA, Taiwan) was used according to standard procedures. Labeled primary antibodies against DDR1 (PA5-29316, Thermo Fisher Scientific In, Waltham, USA), DDR2 (PA5-27752, Thermo Fisher Scientific In, Waltham, USA), Ki67 (AB9260, Millipore, Burlington, MA, USA), proliferating cell nuclear antigen (PCNA) (ARG62605, Arigo Biolaboratories Corp.), active caspase-3 (ab49822, Abcam Inc, Cambridge, MA, USA), Sox9 (AB5535, Millipore, Burlington, MA, USA), Col-II (ab34712, Abcam Inc, Cambridge, MA, USA), Ihh (ab39634, Abcam Inc, Cambridge, MA, USA), Col-X (LB-0092, Cosmo Bio Co LTD, Tokyo), and Runx2 (ORB10256, Biorbyt LLC Ltd, San Francisco, CA, USA), MMP13 (ab39012, Abcam Inc, Cambridge, MA, USA) were incubated with the sections at 4°C overnight. After a final counterstaining with hematoxylin (MHS1-100ML, Sigma-Aldrich, St. Louis, MO, USA), the slides were observed with a Leica-DM1000 microscope (Leica Microsystems, Wetzlar, Germany). For TissueQuest analysis, images were converted to an 8-bit JPEG file with a size of less than 3200x1400 pixels. The same threshold was set in a 0.12-mm^2 area to analyze the DAB intensity. Each group contained more than six independent samples.

2.9 | Quantitative real-time PCR analysis

Long bone cartilage from *Ddr1*$^{f/f\text{-}4OHT}$ or CKOΔ*Ddr1* mice were extracted at P4-P5 and placed on ice. Total RNA was extracted with TRIzol (Thermo Fisher Scientific In, Waltham, USA), and 2 μg cDNA was transcribed from total RNA using the SuperScript II First-Strand Synthesis System (Invitrogen, Carlsbad, CA). For qPCR analysis, a Perkin-Elmer Gene Amp 9700 PCR system (Applied Biosystems, Branchburg, NJ, USA) was used, and a 13 μL reaction solution was prepared with 6.25 μL of SYBR Green Real-Time PCR Master Mix (A25743, Thermo Fisher Scientific In, Waltham, USA) containing 100 nM primer (Table 1) and 1 μL of cDNA; the samples were run on a CFX connect Real-Time PCR detection system (Bio-Rad).

2.10 | Western blot analysis

Cell lysate was extracted from long bone cartilage of P4-P5 *Ddr1*$^{f/f\text{-}4OHT}$ and CKOΔ*Ddr1* mice into lysis buffer (RIPA buffer; 150 mM NaCl, 1 mM EGTA, 50 mM Tris, pH 7.4, 10% glycerol, 1% Triton X-100, 1% sodium deoxycholate, 0.1% SDS) containing 1% of proteinase inhibitor cocktail (Sigma-Aldrich, St. Louis, MO, USA). Western blot was performed using antibodies against DDR1, Ihh, Col-X, GAPDH (MA5-15738, Thermo Fisher Scientific In., Waltham, USA), Gli1 (ab49314, Abcam Inc, Cambridge, MA, USA), and Gli2 (ab167389, Abcam Inc, Cambridge, MA, USA); protein bands were then detected by enhanced chemiluminescence analysis (ECL system; GE Healthcare, Piscataway, NJ, USA).

2.11 | BrdU injections

The BrdU labeling reagent (In situ cell proliferation kit; Sigma-Aldrich, St. Louis, MO, USA) was dissolved in saline with the concentration of 10 μg/1 μL. Each mouse was injected with 10 μg/1 g/1 μL. Intraperitoneal injection the BrdU labeling reagent at 1-week-old mice before 3 hours sacrificed.

TABLE 1 Primer list for RT-PCR

Gene symbol	Forward		Reversed	
DDR1	**5′**	**GCTGTCTGCAGAGGGAGAT**	**3′**	**AAGAGTAGCAGCAGCAGTAG**
DDR2	5′	GAGGAGGAGCGGGGAC	3′	GGATCTGGAGTATCAGAGGG
MMP-13	5′	CCACGTGTGGAGTTATGATG	3′	ACAGCATCTACTTTGTTGCC
RUNX2	5′	GCTCTGGCGTTTAAATGGTT	3′	GCTTGCAGCCTTAAATATTCCT
SOX9	5′	CTCTGGAGGCTGCTGAAC	3′	TGGTACTTGTAATCGGGGTG
ColII	5′	GTGACACTGGGAATGTCCTC	3′	TTTGGCCCTAATTTTCCACTG
ColX	5′	CTCCCAGCACCAGAATCTA	3′	CGTTCAGCATAAAACATCCCA

2.12 | Transferase dUTP nick end labeling staining

Apoptotic cells in cartilage tissues were detected by terminal deoxynucleotidyl transferase dUTP nick end labeling (TUNEL) assay with an In Situ Cell Death Detection Kit (ab206386, Abcam Inc, Cambridge, MA, USA) according to the manufacturer's protocol. Stained cells were observed under a Leica-DMi8 microscope (Leica Microsystems, Wetzlar, Germany). For quantification of TUNEL-positive cells, the number of red cells in six fields was counted using Image-Pro Plus.

2.13 | Statistical analysis

Each experiment was repeated at least three times, and those data are expressed as the means ± standard error of the mean (SEM) of the combined data from each experimental replicate. Statistical significance was evaluated by Student's *t* test, and multiple comparisons were performed using Scheffe's method. (*), (**), and (***) indicate $P < .05$, $P < .01$, and $P < .001$, respectively, and were considered significant.

3 | RESULTS

3.1 | Skeletal dysplasia of chondrocyte-specific (a1(II) collagen CreERT;*Ddr1*$^{f/f}$ mice) CKOΔ*Ddr1* mice

To evaluate the distribution of DDR1 expression in the tibias growth plate, we performed immunohistochemistry (IHC) staining of DDR1. The results showed that DDR1 was expressed in the proliferation zone (PZ) (arrow) and hypertrophic zone (HZ) (arrow) of 1-week-old *Ddr1*$^{f/f\text{-}4OHT}$ mice (Figure S1B), which suggested that DDR1 may play a role in regulating chondrocytes during endochondral ossification. To avoid the limitations of global *Ddr1* knockout, we used inducible chondrocyte-specific *Ddr1* knockout mice (a1(II)-CreERT;*Ddr1*$^{f/f}$; CKO mice) and investigated the development of growth plates during skeletal development. The presence of a floxP site at 730 bp and an a1(II)-CreERT site at 530 bp (Figure S1C) indicated the CKO mice. qPCR analysis of the tissue-specific *Ddr1* knockout in CKOΔ*Ddr1* mice showed that *Ddr1* gene expression was decreased by more than 99.9% in CKOΔ*Ddr1* mice (Figure 1B), with no change in *Ddr2* expression (Figure S1D). DDR1 protein levels decreased by approximately 92% in CKOΔ*Ddr1* mice (Figures 1D and S1E). The IHC results showed obvious DDR1 staining in the muscle (arrow) and bone marrow (arrow), but undetectable staining in the cartilage of 1-week-old CKOΔ*Ddr1* mice (Figure 1D). Meanwhile, DDR2 levels in cartilage, muscle, and bone marrow did not differ between *Ddr1*$^{f/f\text{-}4OHT}$ and CKOΔ*Ddr1* mice (Figure S1F). These results indicated the successful creation of (CKOΔ*Ddr1*) mice exhibiting a *Ddr2*-independent expression pattern in CKOΔ*Ddr1* mice. In E18.5 day mice, *Ddr1* knockout in chondrocytes showed no significant difference in body length (Figure S1G,H), but decreasing the body weight in CKOΔ*Ddr1* mice (Figure S1I). And the results showed that knockout *Ddr1* in chondrocytes decrease the body length and weight from 1- to 12-week-old CKOΔ*Ddr1* mice (Figure 1E). These results indicated *Ddr1* regulated the body length and weight at postnatal during skeletal development without attenuated with age in CKOΔ*Ddr1* mice. According to micro-CT analysis, the body length has no significant difference between Ddr1$^{f/f\text{-}4OHT}$ male/female, and CKOΔ*Ddr1* male/female mice at 4-week-old mice (Figure S3A). However, at 8 weeks of age, CKOΔ*Ddr1*-female mice were significant decreases in body length and weight than that of Ddr1$^{f/f\text{-}4OHT}$-male/female and CKOΔ*Ddr1* male (Figure S3A). This result shows that CKOΔ*Ddr1*-female mice has greater decreasing body length and weight with age. To characterize the role of *Ddr1* during skeletogenesis, we performed double staining in which mineralized matrix appeared purple and cartilaginous matrix appeared blue. The 1- and 2-week-old CKOΔ*Ddr1* mice showed short stature than *Ddr1*$^{f/f\text{-}4OHT}$ mice (Figure 1F), In particular, CKOΔ*Ddr1* mice had smaller endochondral ossification bones (vertebrae, scapula and forelimb, hind limb) (Figure 1G) and intramembranous ossification bones (calvarial, mandibular, clavicle, rib and sternum) (Figure S1J) than *Ddr1*$^{f/f\text{-}4OHT}$ mice. The quantitative lengths of long bones, including humerus, ulna, radius, femur, and tibia, were significantly decreased in 4-week-old CKOΔ*Ddr1* mice (Figure 1H). These findings indicated that *Ddr1* knockout in chondrocytes causes skeletal dysplasia in postnatal mice and suggested that DDR1 can regulate chondrocyte function during the progression of skeletogenesis.

3.2 | Delayed development of the secondary ossification center occurs in the hindlimbs of CKOΔ*Ddr1* mice

The diaphysis of the long bone is the primary ossification center (POC), and each end of the epiphysis has secondary ossification centers (SOCs). Between the epiphysis and metaphysis is the growth plate. The growth plate is the major site driving expansion of the ossification center.[20,21] The double staining results shown in Figure 2A show the SOCs (black arrow) of the femur (yellow dot circle) and tibia (red dot circle) in *Ddr1*$^{f/f\text{-}4OHT}$ mice for 1 week, with more complete development in 2-week-old mice. By contrast, CKOΔ*Ddr1* mice (Figure 2A) showed a lack of or a small SOC (N = 4) in 1-week-old mice and delayed development of the SOC in 2-week-old mice. Furthermore, in the reconstructed

3-D images of cross-sectional views of 4-week-old tibiae (Figure 2B), we observed that the average length of the tibial growth plate (Figure 2B, arrow) was significantly increased in CKOΔ*Ddr1* mice (Figure 2C). This result indicated that *Ddr1* knockout in chondrocytes delayed the development of SOCs and increased the growth plate length. To investigate whether *Ddr1* knockout in chondrocytes affected the growth plate, we used safranin O staining to stain for GAG (Figure 2D). The safranin O staining showed that there was no growth plate difference in tibias of E18.5 day mice but longer in postnatal CKOΔ*Ddr1* mice (Figure S3B). The PZ of the growth plate consists of four to eight flattened and spindle-shaped chondrocytes that form longitudinal columns toward the HZ,[22,23] and the HZ comprises growth plate chondrocytes undergoing hypertrophy along the axis of the long bone. Then, the cell size increased, and apoptosis permitted endochondral ossification.[24] The length of the PZ and HZ in H&E-stained tibial growth plates from $Ddr1^{f/f\text{-}4OHT}$ mice was measured (Figure 2E). But quantification of H&E-stained showed that the length of the growth plate in the tibiae was longer in 2- and 4-week-old CKOΔ*Ddr1* mice than in $Ddr1^{f/f\text{-}4OHT}$ mice (Figure 2F). The PZ length did not change in 1-week-old CKOΔ*Ddr1* mice but was significantly increased in 2- and 4-week-old CKOΔ*Ddr1* mice (Figure 2G). The HZ length was significantly increased in 2-week-old CKOΔ*Ddr1* mice (Figure 2H). Compared with chondrocytes from $Ddr1^{f/f\text{-}4OHT}$ mice, the chondrocytes from CKOΔ*Ddr1* mice were arranged irregularly and had a collapsed longitudinal column, which indicates disorganized chondrocyte arrangement in the HZ of the growth plate (Figure 2I). In CKOΔ*Ddr1* mice, the quantitative results showed increased chondrocyte size in the HZ but not in the PZ (Figure 2J), and increased chondrocyte number in the PZ (Figure 2K). These findings indicated that *Ddr1* knockout in chondrocytes caused cell accumulation in the PZ and increased cell size in the HZ, which caused the growth plate length to expand.

3.3 | Decreased chondrocyte proliferation and apoptosis in the growth plates of CKOΔ*Ddr1* mice

Because there were accumulated chondrocytes in the PZ of the growth plate in CKOΔ*Ddr1* mice, we further analyzed whether the proliferating chondrocytes in the growth plate were altered in CKOΔ*Ddr1* mice. BrdU labeling reagent was IP injected in 1-week-old mice and then detected the BrdU positive cells in growth plate of tibia. The results showed that the proliferating cells in CKOΔ*Ddr1* mice were significantly decreased than in $Ddr1^{f/f\text{-}4OHT}$ mice (Figure 3A-D). Ki67 and PCNA are also proliferation markers, and the qPCR results showed that Ki67 and PCNA expression was downregulated in CKOΔ*Ddr1* mice (Figure S2A). The IHC results also showed less Ki67 staining in the PZ of CKOΔ*Ddr1* mice than $Ddr1^{f/f\text{-}4OHT}$ mice (Figure 3E). Quantification of Ki67 staining intensity revealed significantly decreased Ki67 expression in the PZ of CKOΔ*Ddr1* mice (Figure S2B). Moreover, PCNA staining was also decreased in the PZ of CKOΔ*Ddr1* mice (Figure 3E). Quantification of the PCNA intensity indicated an approximately 52% decrease in PCNA levels in CKOΔ*Ddr1* mice (Figure S2B). The data showed that knockout *Ddr1* in chondrocyte reduced the cell proliferation. The results indicated that *Ddr1* regulated chondrocyte proliferating functions during skeletal development. To investigate whether *Ddr1* knockout in chondrocytes affects apoptosis, we evaluated apoptotic chondrocytes by analyzing caspase-3. Caspase-3 expression was markedly reduced in the HZ of 1-week-old CKOΔ*Ddr1* mice compared with age-matched $Ddr1^{f/f\text{-}4OHT}$ mice (Figure 3F). Quantification of the staining intensities showed that caspase-3 was significantly decreased by approximately 96% in CKOΔ*Ddr1* mice (Figure S2B). Next, we investigated whether *Ddr1* knockout in chondrocytes prevented cell apoptosis in the growth plate. The number of apoptotic chondrocytes decreased in HZ (yellow square; yellow arrow) in 1-week-old CKOΔ*Ddr1* mice (Figure 3F). After quantification, the number of TUNEL-positive chondrocytes in the HZ of CKOΔ*Ddr1* mice decreased 64% (Figure 3F), respectively. These results indicated that *Ddr1* knockout in chondrocytes increased the length of the growth plate due to decreased chondrocyte terminal differentiation and cell death.

3.4 | Delayed chondrocyte terminal differentiation in the tibial growth plate of CKOΔ*Ddr1* mice

To investigate whether *Ddr1* knockout in chondrocytes influences chondrogenesis. The qPCR results showed that *Ddr1* knockout in chondrocytes did not significantly affect the gene expression of the chondrogenic marker Sox9 (Figure 4A). Additionally, there was no change in Sox9 in the CKOΔ*Ddr1* mouse growth plate as assessed by the IHC staining and quantitative results at below. (Figure 4B,C). The expression of other chondrogenic genes, such as Col-II was not affected, and IHC staining also showed no difference in the extracellular matrix composition in the growth plates of CKOΔ*Ddr1* and $Ddr1^{f/f\text{-}4OHT}$ mice (Figure 4A-C). Compared to the chondrocytes and osteoblasts from $Ddr1^{f/f\text{-}4OHT}$ mice, the hypertrophic chondrocytes and osteoblasts in CKOΔ*Ddr1* mice required Runx2, a transcription factor, to target the promoter regions of Col-X and MMP-13.[25,26] Runx2 and Mef2C regulate the expression of terminal differentiation markers, including Col-X, Ihh, MMP-13, alkaline phosphatase (ALP), and vascular endothelial growth factor (VEGF), to drive endochondral

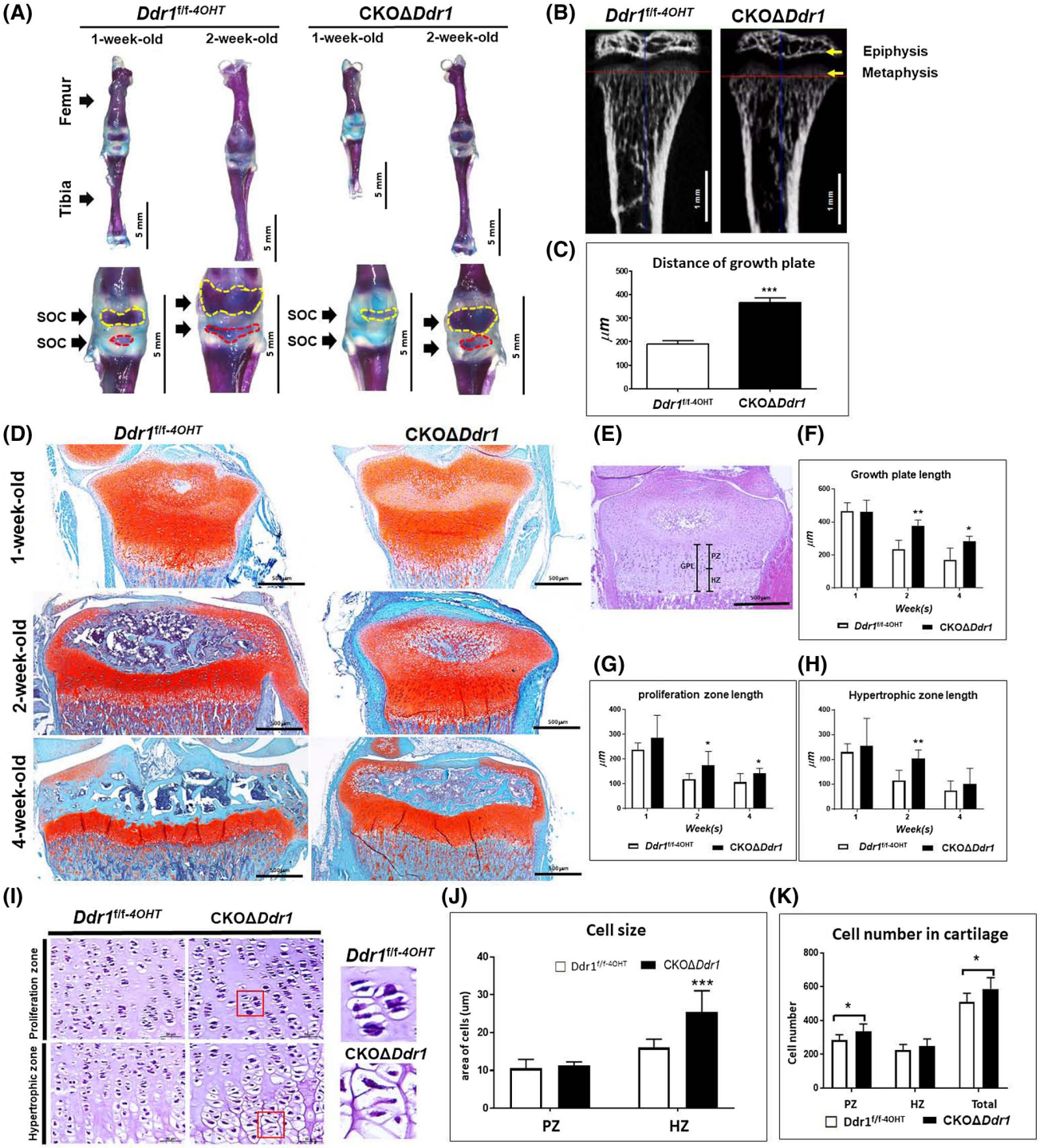

FIGURE 2 Delayed development of the SOC in the Hind limbs of CKOΔ*Ddr1* mice. A, Double staining of femurs and tibiae from 1- and 2-week-old mice. The images represent magnifications of 1.25X (upper) and 2.5X (bottom). SOC (black arrow) at the femur (yellow dot circle) and tibia (red dot circle). Scale bar 5 mm. B, 3-D micro-CT structure of a cross-sectional view of *Ddr1*$^{f/f\text{-}4OHT}$ and CKOΔ*Ddr1* mice. Scale bar 1 mm. C, Image-Pro Plus analysis of the growth plate length between the epiphysis and metaphysis. D, Safranin O & Fast green staining for GAG at 1-, 2-, and 4-week-old tibial growth plates from *Ddr1*$^{f/f\text{-}4OHT}$ and CKOΔ*Ddr1* mice. The magnification was 40X, and the scale bar was 500 μm. E, H&E staining was used to define the proliferation and hypertrophy zones (PZ and HZ, respectively) in 1-week-old *Ddr1*$^{f/f\text{-}4OHT}$ mice. Quantification of the (F) growth plate length (GPL). G, Proliferation zone (PZ) length, and (H) hypertrophy zone (HZ) length by Image-Pro Plus. I, H&E staining for cell morphology in the PZ and HZ of 1-week-old mouse tibiae. The magnification was 400X, and the scale bar is 50 μm. J, The number of chondrocytes in each zone was counted with Image-Pro Plus. K, Quantification of the cell size in the growth plate of each zone as performed with Image-Pro Plus. Each group, N ≥ 6; the data represent the mean ± SE by Student's *t* test; **P* ≤ .05, ***P* ≤ .01, ****P* ≤ .001

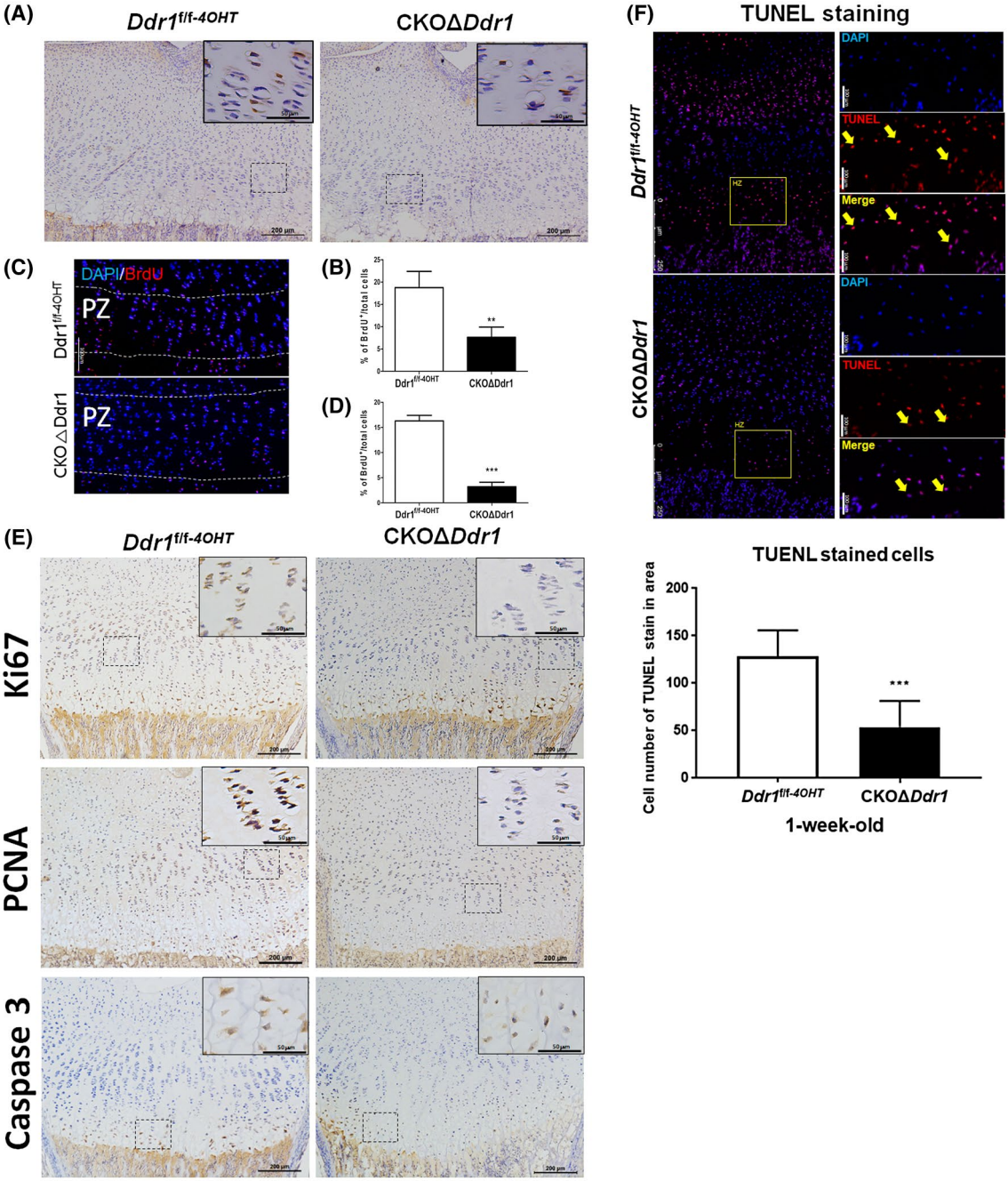

FIGURE 3 Decrease in chondrocyte proliferation and apoptosis in the growth plates of CKOΔ*Ddr1* mice. A, IHC staining of BrdU positive cell in 1-week-old *Ddr1*$^{f/f\text{-}4OHT}$ and CKOΔ*Ddr1* mice tibia growth plate. The BrdU positive cells (brown) at proliferation zone. The magnification was 40X and 100X, and the scale bar was 200 and 50 μm. B, TissueQuest analysis percentage of BrdU^{+} cells/total cells. C, Immunofluorescence of BrdU positive cell in 1-week-old *Ddr1*$^{f/f\text{-}4OHT}$ and CKOΔ*Ddr1* mice tibia growth plate. The BrdU^{+} cells (red) and DAPI (blue), the PZ means proliferation zone. Scale bar 100 μm. D, Image-Pro Plus analysis. Percentage of BrdU^{+} cells/total cells. E, IHC staining of Ki67, PCNA and Caspase 3 in 1-week-old *Ddr1*$^{f/f\text{-}4OHT}$ and CKOΔ*Ddr1* mice. Magnifications of 100X and 400X are shown; the scale bars are 200 and 50 μm, respectively. F, TUNEL staining in the HZ of 1-week-old mice. The magnifications were 100X and 400X, and the scale bars were 250 and 100 μm, respectively. Image-Pro Plus analysis of the number of TUNEL-positive cells/the number of DAPI-stained cells. Each group, $N \geq 6$; the data represent the mean ± SE by Student's *t* test; $^{***}P \leq .001$

ossification.[9,27-29] Ihh, a hypertrophic marker, was significantly decreased in gene expression (Figure 4A) and IHC staining in the HZ (Figure 4B). There was no significant decrease in Runx2 gene expression in the HZ of CKOΔ*Ddr1* mice (Figure 4A), but a decrease in IHC staining intensity was observed (Figure 4B). The terminal differentiation marker Col-X showed decreased gene expression by approximately 90% compared with that in *Ddr1*$^{f/f\text{-}4OHT}$ mice

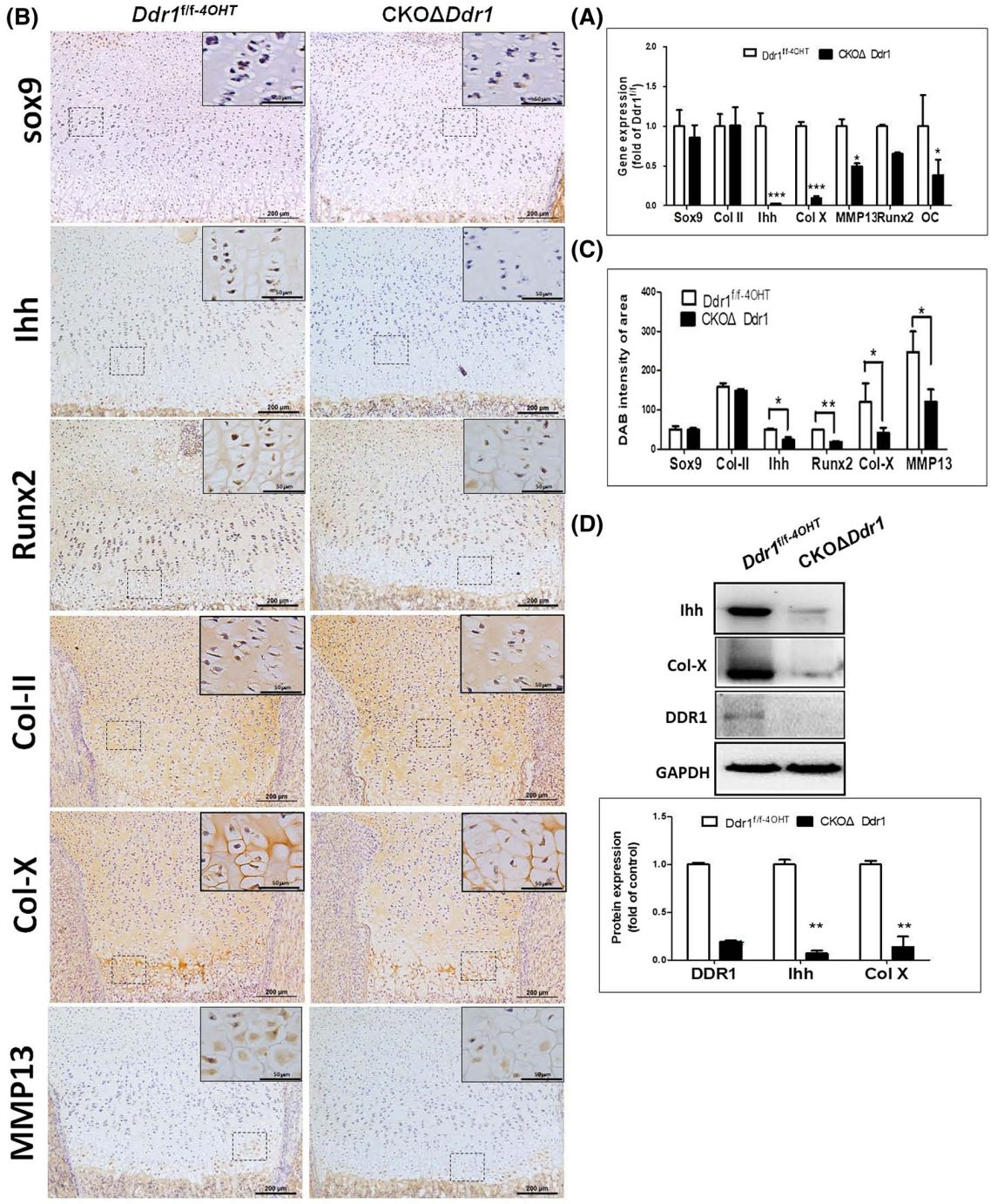

FIGURE 4 Delayed chondrocyte terminal differentiation in the tibial growth plate of CKOΔ*Ddr1* mice. A, Gene expression of Sox9, Col-II, Ihh, Col-X, MMP13, Runx2, and OC in tibiae extracted from P4-P5 $Ddr1^{f/f\text{-}4OHT}$ and CKOΔ*Ddr1* mice. IHC staining of (B) Sox9 and Ihh, Runx2, Col-II, Col-X, and MMP13 in $Ddr1^{f/f\text{-}4OHT}$ and CKOΔ*Ddr1* mice. Magnifications of 100X and 400X are shown, with scale bars of 200 and 50 μm. C, Quantification of IHC staining intensity by TissueQuest. The protein expression of (D) Ihh, Col-X, and DDR1 was assessed in articular cartilage extracted from P4-P5 mice. The quantitative results are shown below. Each group, N ≥ 6; the data represent the mean ± SE by Student's *t* test; $*P \leq .05$, $**P \leq .01$, $***P \leq .001$

(Figure 4A); moreover, the IHC staining was also decreased in the HZ of CKOΔ*Ddr1* mice (Figure 4B). Another hypertrophic marker MMP13, was showed with 42% gene expression, as well as the IHC staining decreased in the HZ of CKOΔ*Ddr1* mice (Figure 4B). After the IHC staining was quantified, the results showed that Ihh, Runx2, Col-X, and MMP13 were significantly decreased in CKOΔ*Ddr1* mice (Figure 4C). We also detected a decrease in the gene expression of osteocalcin (OC) in CKOΔ*Ddr1* mice (Figure 4A). Apparently, Ihh and Col-X protein levels were downregulated in CKOΔ*Ddr1* mice (Figure 4D). These results indicated that knocking out *Ddr1* in chondrocytes may decrease

chondrocyte hypertrophy and result in delayed terminal differentiation and endochondral ossification.

3.5 | Reduced endochondral bone ossification in tibia of CKOΔ*Ddr1* mice

To investigate whether delayed endochondral ossification progression in CKOΔ*Ddr1* mice influences bone calcification formation, we used micro-CT analysis. In the tibiae from 4-week-old mice, the reconstructed 3-D images, and coronal section of the views of CKOΔ*Ddr1* mice revealed thinner tibiae than those in *Ddr1*$^{f/f\text{-}4OHT}$ mice (Figure 5A). Micro-CT showed that the tibiae in CKOΔ*Ddr1* mice had a significantly decreased BV/TV ratio (Figure 5B) and Tb, Th (Figure 5C), but there was no significant difference in Tb, N (Figure 5D), and Tb, Sp (Figure 5E). The cortex thickness was analyzed in the middle of the diaphysis, with total 2 mm, and a cross-sectional view of the micro-CT 3-D structure was analyzed (Figure 5F). The results showed that CKOΔ*Ddr1* mice had no effect on cortex thickness compared with *Ddr1*$^{f/f\text{-}4OHT}$ mice (Figure 5G). These findings indicate that *Ddr1* knockout in chondrocytes influences endochondral ossification.

3.6 | DDR1 regulates chondrocyte terminal differentiation through the Ihh/Gli1/Gli2/Col-X pathway

In this study, chondrocyte with *Ddr1* knockout decreased chondrocyte terminal differentiation, resulting in delayed endochondral ossification. We demonstrated that terminal differentiation markers were significantly decreased in CKOΔ*Ddr1* mice. Ihh was previously reported to positively regulate Col-X expression. The Ihh downstream signaling molecules Gli1/2 together with Runx2/Smads regulate the transcription and expression of Col-X.[30] To investigate the detailed mechanism by which *Ddr1* regulates chondrocyte terminal differentiation, we used lentivirus knockdown/overexpression of *Ddr1* in chondrosarcoma SW1353 cells and HAC to evaluate the mechanism of *Ddr1* in human chondrocytes. Our results showed that lentivirus knockdown of *Ddr1* in SW1353 cells affected protein levels of Ihh and the downstream molecules Gli1/Gli2/Col-X (Figure 6A,B) Moreover, overexpression of *Ddr1* in SW1353 cells were increased Ihh and Gli1/Gli2/Col-X protein level (Figure 6C). To investigate whether *Ddr1* regulates Col-X through the Ihh/Gli1/Gli2 pathway, we performed overexpression of *Ddr1* and treated with Ihh inhibitor HPI-4 for 24 hours. The results showed that Gli1/Gli2/Col-X protein levels were increased in cells overexpressing *Ddr1* but decreased in *Ddr1*-overexpressing cells co-treated with HPI-4 (Figure 6D). These results indicate that *Ddr1* regulated chondrocyte hypertrophy through the Ihh/Gli1/Gli2/Col-X pathway.

4 | DISCUSSION

In this study, we generated novel *Ddr1*$^{f/f\text{-}4OHT}$ mice with floxed exon 2 and exon 12 of the DDR1 locus. DDR1 is composed of 17 exons; exons 1-8 encode the extracellular discoidin domain (DS), including discoidin domains 1 and 2, in which the N-terminal region (discoidin 1) recognizes various collagens as a binding site, exon 9 encodes the transmembrane domain (TM), and exons 10-12 encode the cytosolic juxtamembrane (JM). In CKOΔ*Ddr1* mice, truncation of exons 2 to 12 of the DDR1 locus inactivates DDR1 tyrosine kinase, and the knockout of *Ddr1* appears to be chondrocyte-specific. Endochondral ossification is a process of differentiation from mesenchymal stem cells into chondrocytes, which in growth plates promote longitudinal growth of long bones. In this study, we observed delayed development of the SOC and increased growth plate length in the hind limbs of CKOΔ*Ddr1* mice. Chondrocytes with *Ddr1* knockout presented abnormal development of the growth plate and delayed endochondral ossification. We demonstrated that chondrocytes with *Ddr1* knockout exhibited decreased proliferation, terminal differentiation, and apoptosis at growth plates. Knockout of *Ddr1* in chondrocytes did not influence Sox9 and Col-II expression but reduced Ihh, Runx2, Col-X, and MMP13 expression in CKOΔ*Ddr1* mice. Notably, the molecular mechanism by which *Ddr1* knockout decreased chondrocyte terminal differentiation involved the Ihh/Gli1/Gli2/Col-X pathway. Therefore, our results indicated that *Ddr1* is required in chondrocytes for endochondral ossification by regulating the proliferation, terminal differentiation, and apoptosis of chondrocytes during skeletal development.

In the growth plate, chondrogenesis requires chondrocyte proliferation, hypertrophy, and apoptosis, with gradually remodeling of the cartilage into bone. There have been no reports a role of *Ddr1* in chondrocytes during endochondral ossification. Here, we identified a crucial role of *Ddr1* in chondrocytes by promoting growth plate development. This difference in growth plate length was due to reduced chondrocytes proliferation, hypertrophy, and apoptosis, which resulted in the accumulation of chondrocytes in the growth plate. Interestingly, our results also showed that intramembrane ossification was suppressed in chondrocytes with *Ddr1* knockout. A previous report showed Col2a1-directed expression of Cre recombinase in cranial mesenchymal stem cells at embryonic day 11.5.[31] Interestingly, our results also showed that intramembrane ossification was suppressed in chondrocytes with *Ddr1* knockout. These results suggest that *Ddr1* knockout in chondrocytes interferes with the process of intramembrane ossification.

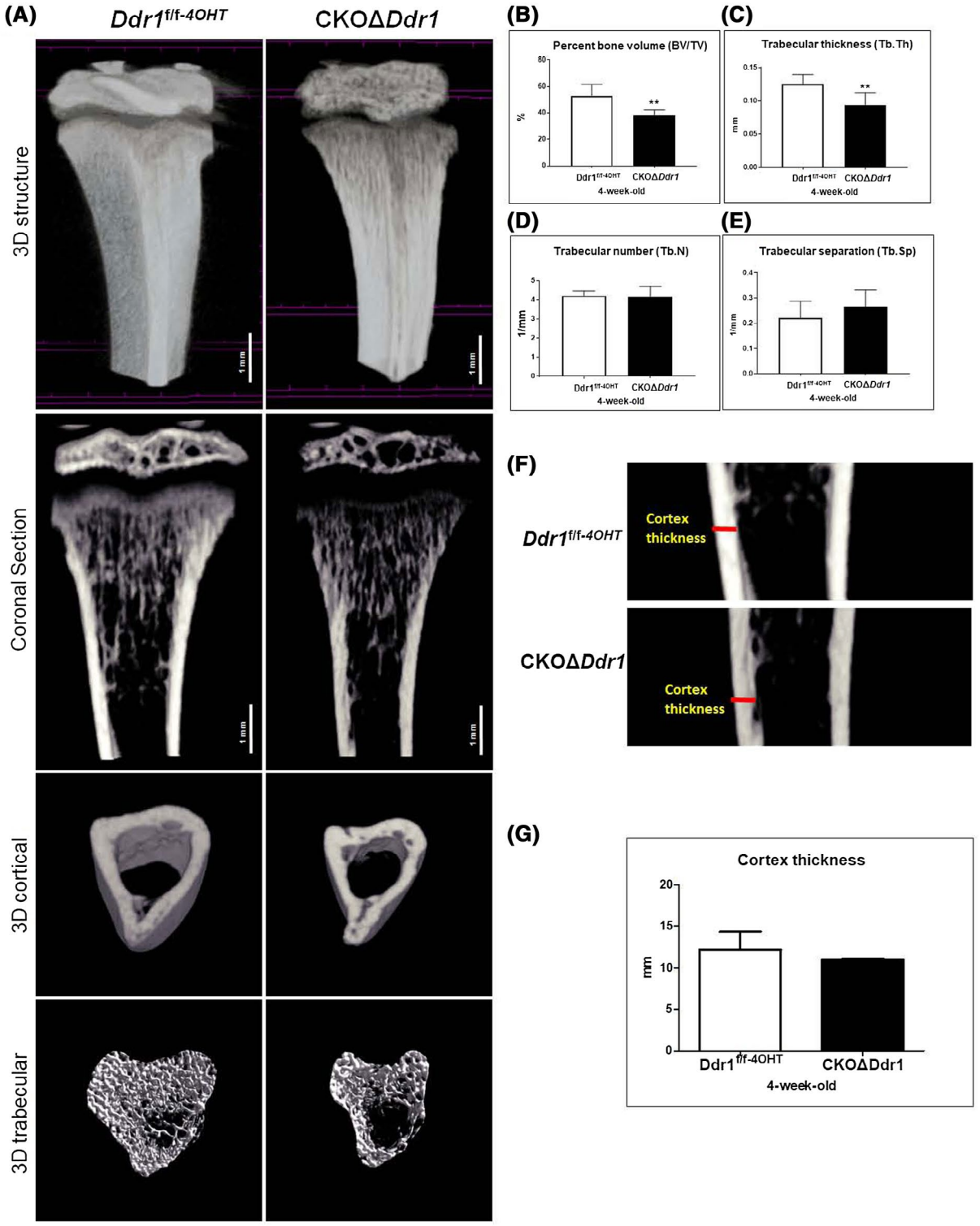

FIGURE 5 Reduced endochondral bone ossification in tibia of CKOΔ*Ddr1* mice. Micro-CT was used to (A) construct the 3-D structure and coronal section of 5 mm tibia, and 3-D cortical and 3-D trabecular of 2 mm in 4-week-old mice. Scale bar, 1 mm. B, Percentage bone volume (BV/TV). C, Trabecular thickness (Tb.Th). D, Trabecular number (Tb.N). E, Trabecular separation. (Tb.Sp). F, Micro-CT image showing the cortex beneath growth plate 5.0-7.0 mm (total length 2 mm) of the diaphysis. G, Image-Pro Plus analysis of the cortex thickness. Each group, N ≥ 6; the data represent the mean ± SE by Student's *t* test; $*P \leq .05$, $**P \leq 001$, $***P \leq .001$

In this study, we showed that the expression of Ihh, Col-X, and MMP13, markers of chondrocyte terminal differentiation, were decreased in CKOΔ*Ddr1* mice. Consistent with our results, a previous report indicated that knocking out Runx2 in chondrocytes reduced chondrocyte proliferation activity but did not affect Sox9 and Col-II expression.[32] Targeted

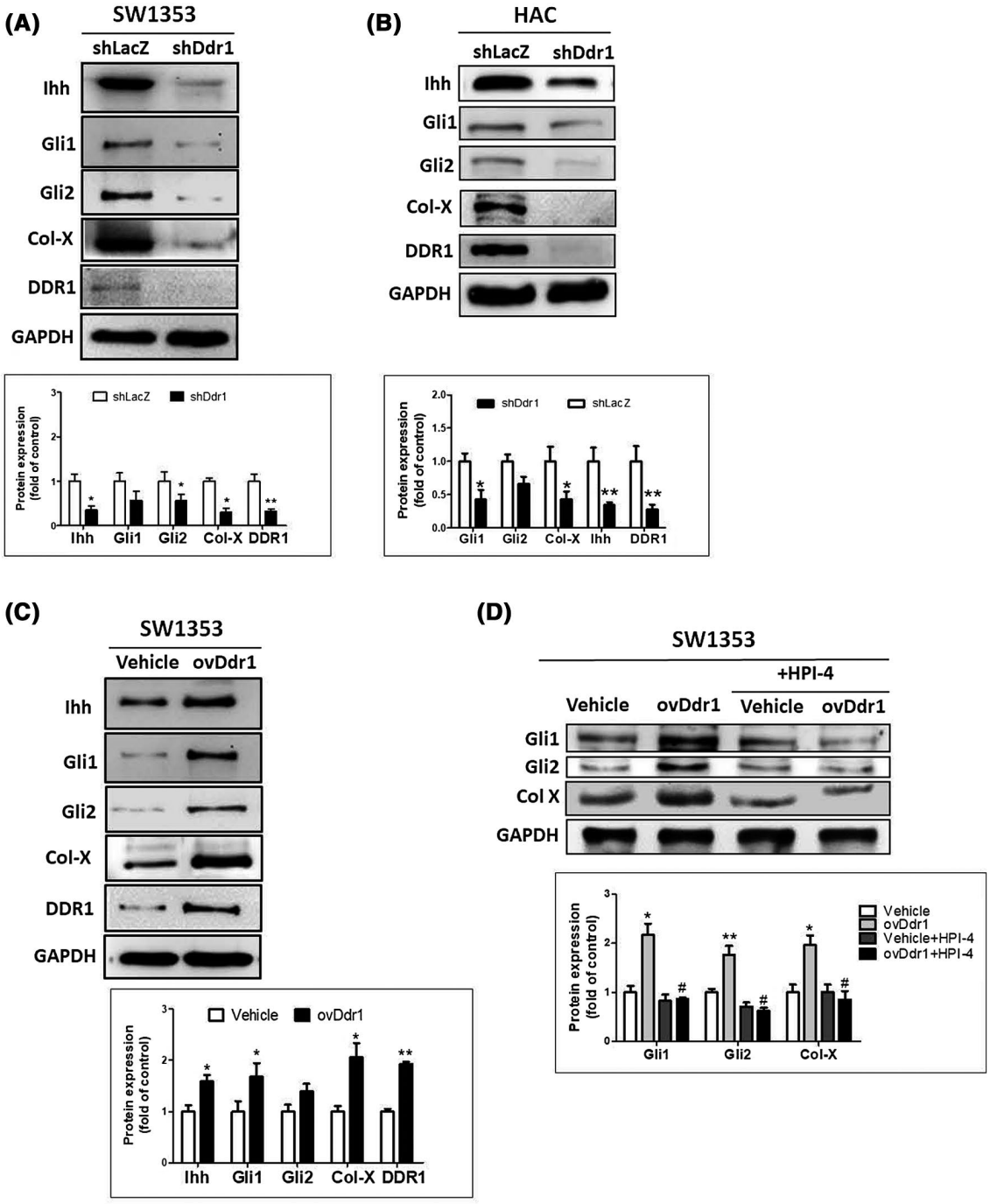

FIGURE 6 DDR1 regulates chondrocyte terminal differentiation through the Ihh/Gli1/Gli2/Col-X pathway. A, *Ddr1* was knocked down in SW1353 cells by lentiviral transfection, and protein levels of Ihh, Gli1, Gli2, Col-X, DDR1, and GAPDH were assessed. The quantitative results are shown below. B, *Ddr1* was knocked down in HAC cells by lentiviral transfection, and protein levels of Ihh, Gli1, Gli2, Col-X, DDR1, and GAPDH were assessed. The quantitative results are shown below. C, *Ddr1* was overexpressed in SW1353 cells by lentiviral transfection, and protein levels of Ihh, Gli1, Gli2, Col-X, DDR1, and GAPDH were assessed. The quantitative results are shown below. D, *Ddr1* was overexpressed in SW1353 cells, and the cells were treated with 10 μM of Ihh inhibitor (HPI-4) for 24 h Gli1, Gli2, and Col-X protein levels were detected. The quantitative results are shown below. Each group, N ≥ 3; the data represent the mean ± SE by Student's *t* test; $*^{\#}P \leq .05$, $**P \leq .01$, * means *ovDdr1* compare with Vehicle, and # means *ovDdr1* + HPI-4 compare with *ovDdr1*

deletion of both Ihh ($Ihh^{-/-}$) and Runx2 ($Runx2^{\Delta E8/\Delta E8}$) in chondrocytes caused short limbs and dwarfism.[32,33] By contrast, Ihh overexpression promoted Runx2 expression and induced Col-X transcriptional activity through Glioma-associated oncogene homolog members (Gli) 1/2, resulting in chondrocyte maturation.[30] Accordingly, we suggest that *Ddr1* in chondrocytes may upregulate Ihh and that the molecules downstream of Runx2 and Gli1/2 affect Col-X and

cause chondrocyte terminal differentiation. To determine the molecular signaling underlying the decrease in chondrocyte terminal differentiation induced by *Ddr1* knockout, we used lentivirus knockdown *Ddr1* in SW1353 cells and HAC cells. Both SW1353 cells and HAC cells with *Ddr1* knockdown decreased Ihh/Gli1/Gli2/Col-X protein levels. We demonstrated that *Ddr1* promotes chondrocyte terminal differentiation via Ihh and the downstream Gli1/Gli2/Col-X signaling pathway. However, the detailed mechanism by which *Ddr1* regulates the expression of Ihh in chondrocytes remain undefined. Inhibition of p38 MAP kinase has been reported to delay chondrocyte hypertrophic differentiation by downregulating the transcription factor myocyte enhancer factor-2c (Mef2c), resulting in a decrease in Col-X expression.[34] Moreover, myocyte enhancer factor-2c (Mef2c) also regulates Col-X expression through MEF2 binding sites in the Col-X promoter, which are antagonized by the co-repressor histone deacetylase 4 (HDAC4).[35] We propose that *Ddr1* potentially mediates chondrocyte terminal differentiation through P38 MAP kinase and that Mef2c regulates Col-X expression.

In this study, we provide the first theoretical basis for explaining how global *Ddr1* knockout causes short stature. By used CKOΔ*Ddr1* mice, we showed that *Ddr1* knockout in chondrocytes also causes short stature and decreases body length/weight, but no other developmental abnormalities were observed. We demonstrated that *Ddr1* knockout in chondrocytes decreases cell proliferation, terminal differentiation, and apoptosis resulting in increased growth plate length and delayed endochondral ossification is responsible for the short stature in CKOΔ*Ddr1* mice. However, Vogel et al reported that global *Ddr1* knockout mice showed short stature with thinner fibular bone, there is no influence on the chondrocyte proliferation and cell death during skeletal development.[32] We propose that the difference between our study and the study of Vogel et al, such as differences in the growth plate, chondrocytes proliferation, and chondrocytes apoptosis, maybe cause by the compensatory effect of *Ddr2* and cross talk of development abnormalities observed in global *Ddr1* knockout mice. Schminke et al, reported that the expression of DDR2 was increased in chondrocytes of the temporomandibular joint from globe *Ddr1* knockout mice, which indicated a compensatory effect of DDR2 in mice with global *Ddr1* knockout.[35] In our study, we showed that specific *Ddr1* knockout in chondrocytes did not influence *Ddr2* expression, which indicated that DDR2 does not exert a compensatory effect on skeletal development in CKOΔ*Ddr1* mice. In addition, CKOΔ*Ddr1* mice without the developmental abnormalities that showed in global *Ddr1* knockout mice, including lactation impairment, reproduction defects,[32] proteinuria,[33] cochlear duct defect, and loss of auditory function.[34]

Previously reported that high dose (100 mg/kg/4 days) of 4-OHT increased the bone mineral density in Col1-CreERT2 young male mice, but no influence was found in the lower doses (≤10 mg/kg/4 day). In this study, we used the lower dosage (4 mg/kg) of 4-OHT, which the results showed at age of 4-week-old were no difference in skeletal phenotype, sGAG content of growth plate, body weight, and length both male and female mice in each of groups ($Ddr1^{f/f\text{-}Oil}$, $Ddr1^{f/f\text{-}4OHT}$, Cre^{+Oil}, and Cre^{+4OHT} mice) during development (data not shown). Therefore, in this study, we used $Ddr1^{f/f\text{-}4OHT}$ as the control group to clarify the delayed mechanism of CKOΔ*Ddr1* during skeletal development.

In conclusion, we demonstrated that *Ddr1* knockout in chondrocytes first decrease Ihh/Gli1/2/Col-X signaling and cause decreases in cell terminal differentiation and apoptosis, resulting in increased growth plate length and delayed endochondral ossification; the delayed ossification of long bones is responsible for the short stature. These results indicated that DDR1 is required for chondrocytes during endochondral ossification. Our findings also provide information for understanding the mechanism of idiopathic dwarfism and cartilaginous diseases, such as osteoarthritis or cartilage hypoplasia.

ACKNOWLEDGMENTS

In this study, the authors acknowledge were grant support by the National Science Council (MOST108-2320-B-037-008) of Chau-Zen Wang; Kaohsiung Medical University (KMU-TP-105B10 and KMU-DK105009) and National Science Council (MOST108-23214-B-037-059) of Chun-Hwan Chen; Orthopaedic Research Center and Regeneration Medicine and Cell Therapy Research Center in Kaohsiung Medical University grand for the research resource and equipment. This study is supported partially by Kaohsiung Medical University Research Center Grant (KMU-TC108A02).

CONFLICT OF INTEREST

The authors report no conflicts of interests.

AUTHOR CONTRIBUTIONS

M.-L. Ho, C.-Z. Wang, C.-H. Chen conceived and designed the study; L.-Y. Chou, Y.-H. Lin, S.-C. Chuang, H.-C. Chou, S.-Y. Lin, Y.-C. Fu, and J.-K. Chang performed experiments and data analysis and interpretation; L.-Y. Chou, M.-L. Ho, C.-Z. Wang drafted the manuscript.

REFERENCES

1. Vogel WF, Abdulhussein R, Ford CE. Sensing extracellular matrix: an update on discoidin domain receptor function. *Cell Signal*. 2006;18(8):1108-1116.
2. Henry SP, Liang S, Akdemir KC, de Crombrugghe B. The postnatal role of Sox9 in cartilage. *J Bone Miner Res*. 2012;27(12):2511-2525.
3. Loebel C, Czekanska EM, Bruderer M, Salzmann G, Alini M, Stoddart MJ. In vitro osteogenic potential of human mesenchymal stem cells is predicted by Runx2/Sox9 ratio. *Tissue Eng Part A*. 2015;21(1–2):115-123.

4. Zhou G, Zheng Q, Engin F, et al. Dominance of SOX9 function over RUNX2 during skeletogenesis. *Proc Natl Acad Sci U S A*. 2006;103(50):19004-19009.
5. Harrington EK, Coon DJ, Kern MF, Svoboda KKH. PTH stimulated growth and decreased Col-X deposition are phosphotidylinositol-3,4,5 triphosphate kinase and mitogen activating protein kinase dependent in avian sterna. *Anat Rec (Hoboken)*. 2010;293(2):225-234.
6. Stickens D, Behonick DJ, Ortega N, et al. Altered endochondral bone development in matrix metalloproteinase 13-deficient mice. *Development*. 2004;131(23):5883-5895.
7. Dreier R. Hypertrophic differentiation of chondrocytes in osteoarthritis: the developmental aspect of degenerative joint disorders. *Arthritis Res Ther*. 2010;12(5):216.
8. St-Jacques B, Hammerschmidt M, McMahon AP. Indian hedgehog signaling regulates proliferation and differentiation of chondrocytes and is essential for bone formation. *Genes Dev*. 1999;13(16):2072-2086.
9. Chen S, Fu P, Cong R, Wu HS, Pei M. Strategies to minimize hypertrophy in cartilage engineering and regeneration. *Genes Dis*. 2015;2(1):76-95.
10. Chen L, Li C, Qiao W, Xu X, Deng C. A Ser(365)–>Cys mutation of fibroblast growth factor receptor 3 in mouse downregulates Ihh/PTHrP signals and causes severe achondroplasia. *Hum Mol Genet*. 2001;10(5):457-465.
11. Mohan RR, Mohan RR, Wilson SE. Discoidin domain receptor (DDR) 1 and 2: collagen-activated tyrosine kinase receptors in the cornea. *Exp Eye Res*. 2001;72(1):87-92.
12. Valiathan RR, Marco M, Leitinger B, Kleer CG, Fridman R. Discoidin domain receptor tyrosine kinases: new players in cancer progression. *Cancer Metastasis Rev*. 2012;31(1–2):295-321.
13. Borza CM, Pozzi A. Discoidin domain receptors in disease. *Matrix Biol*. 2014;34:185-192.
14. Labrador JP, Azcoitia V, Tuckermann J, et al. The collagen receptor DDR2 regulates proliferation and its elimination leads to dwarfism. *EMBO Rep*. 2001;2(5):446-452.
15. Leitinger B. Discoidin domain receptor functions in physiological and pathological conditions. *Int Rev Cell Mol Biol*. 2014;310:39-87.
16. Leitinger B, Steplewski A, Fertala A. The D2 period of collagen II contains a specific binding site for the human discoidin domain receptor, DDR2. *J Mol Biol*. 2004;344(4):993-1003.
17. Leitinger B, Kwan AP. The discoidin domain receptor DDR2 is a receptor for type X collagen. *Matrix Biol*. 2006;25(6):355-364.
18. Schminke B, Muhammad H, Bode C, et al. A discoidin domain receptor 1 knock-out mouse as a novel model for osteoarthritis of the temporomandibular joint. *Cell Mol Life Sci*. 2014;71(6):1081-1096.
19. Nakamura E, Nguyen MT, Mackem S. Kinetics of tamoxifen-regulated Cre activity in mice using a cartilage-specific CreER(T) to assay temporal activity windows along the proximodistal limb skeleton. *Dev Dyn*. 2006;235(9):2603-2612.
20. Pines M, Hurwitz S. The role of the growth plate in longitudinal bone growth. *Poult Sci*. 1991;70(8):1806-1814.
21. Mackie EJ, Ahmed YA, Tatarczuch L, Chen K-S, Mirams M. Endochondral ossification: how cartilage is converted into bone in the developing skeleton. *Int J Biochem Cell Biol*. 2008;40(1):46-62.
22. Li Y, Dudley AT. Noncanonical frizzled signaling regulates cell polarity of growth plate chondrocytes. *Development*. 2009;136(7):1083-1092.
23. Pitsillides AA, Beier F. Cartilage biology in osteoarthritis–lessons from developmental biology. *Nat Rev Rheumatol*. 2011;7(11):654-663.
24. Whitaker AT, Berthet E, Cantu A, Laird DJ, Alliston T. Smad4 regulates growth plate matrix production and chondrocyte polarity. *Biol Open*. 2017;6(3):358-364.
25. Pratap J, Javed A, Languino LR, et al. The Runx2 osteogenic transcription factor regulates matrix metalloproteinase 9 in bone metastatic cancer cells and controls cell invasion. *Mol Cell Biol*. 2005;25(19):8581-8591.
26. Bruderer M, Richards RG, Alini M, Stoddart MJ. Role and regulation of RUNX2 in osteogenesis. *Eur Cell Mater*. 2014;28:269-286.
27. Studer D, Millan C, Öztürk E, Maniura-Weber K, Zenobi-Wong M. Molecular and biophysical mechanisms regulating hypertrophic differentiation in chondrocytes and mesenchymal stem cells. *Eur Cell Mater*. 2012;24:118-135; discussion 135.
28. Yoshida CA, Yamamoto H, Fujita T, et al. Runx2 and Runx3 are essential for chondrocyte maturation, and Runx2 regulates limb growth through induction of Indian hedgehog. *Genes Dev*. 2004;18(8):952-963.
29. Kwon TG, Zhao X, Tang Q, et al. Physical and functional interactions between Runx2 and HIF-1alpha induce vascular endothelial growth factor gene expression. *J Cell Biochem*. 2011;112(12):3582-3593.
30. Amano K, Densmore M, Nishimura R, Lanske B. Indian hedgehog signaling regulates transcription and expression of collagen type X via Runx2/Smads interactions. *J Biol Chem*. 2014;289(36):24898-24910.
31. Ovchinnikov DA, Deng JM, Ogunrinu G, Behringer RR. Col2a1-directed expression of Cre recombinase in differentiating chondrocytes in transgenic mice. *Genesis*. 2000;26(2):145-146.
32. Chen H, Ghori-Javed FY, Rashid H, et al. Runx2 regulates endochondral ossification through control of chondrocyte proliferation and differentiation. *J Bone Miner Res*. 2014;29(12):2653-2665.
33. Karp SJ, Schipani E, St-Jacques B, et al. Indian hedgehog coordinates endochondral bone growth and morphogenesis via parathyroid hormone related-protein-dependent and -independent pathways. *Development*. 2000;127(3):543-548.
34. Stanton L-A, Sabari S, Sampaio AV, Underhill TM, Beier F. p38 MAP kinase signalling is required for hypertrophic chondrocyte differentiation. *Biochem J*. 2004;378(Pt 1):53-62.
35. Kozhemyakina E, Cohen T, Yao T-P, Lassar AB. Parathyroid hormone-related peptide represses chondrocyte hypertrophy through a protein phosphatase 2A/histone deacetylase 4/MEF2 pathway. *Mol Cell Biol*. 2009;29(21):5751-5762.

SUPPORTING INFORMATION

Additional Supporting Information may be found online in the Supporting Information section.

How to cite this article: Chou L-Y, Chen C-H, Lin Y-H, et al. Discoidin domain receptor 1 regulates endochondral ossification through terminal differentiation of chondrocytes. *The FASEB Journal*. 2020;00:1–15. https://doi.org/10.1096/fj.201901852RR